

# Heat Transfer in Injection Molding of Crystalline Plastics

Yu Bai,<sup>1</sup> Bo Yin,<sup>2</sup> Xia-rong Fu,<sup>1</sup> Min-gbo Yang<sup>2</sup>

<sup>1</sup>College of Chemical Engineering, Sichuan University, Chengdu, 610065 Sichuan, People's Republic of China

<sup>2</sup>College of Polymer Science and Engineering, State Key Laboratory of Polymer Materials Engineering, Sichuan University, Chengdu, 610065 Sichuan, People's Republic of China

Received 16 November 2005; accepted 23 February 2006

DOI 10.1002/app.24398

Published online in Wiley InterScience (www.interscience.wiley.com).

**ABSTRACT:** A theoretical mathematical model is presented to describe the temperature distribution and the rate of phase change in the injection molding process of crystalline plastics. Under some assumptions, an exact closed form is solved with the use of an internal technique. The model was tested by measuring the temperature profile in a slab mold instrumented with thermocou-

ples. Measurements of temperature profiles in the center of the polymer slab compare well to model prediction. © 2006 Wiley Periodicals, Inc. *J Appl Polym Sci* 102: 2249–2253, 2006

**Key words:** crystalline plastics; injection molding; heat transfer; cooling

## INTRODUCTION

Heat transfer is one of the most important stages in injection molding process, because the material physical properties, surface quality, and demolding time are largely dependent on thermal change in the mold. Not many exact solutions can be found for these heat transfer problems because of the inherent nonlinearities present. It is very necessary to find a mathematical model for the injection molding of crystalline plastics. This mathematical model could help us understand the cooling process of plastics products in injection molding, optimize the technology of injection molding computer-aided design (CAD), and establish feasible processing conditions.

The cooling process of the plastics product involves phase changes and has special characteristics: the transferred heat contains not only the sensible heat, but also the latent heat released at the interface. The solid–liquid interphase moves with increasing time; as a result, the location of the solid–liquid interface is not known a priori and must be followed as a part of the solution. The problems of phase change due to heat transfer and moving interphase are well recognized.<sup>1–5</sup> Investigations of the heat transfer of crystalline plastics in injection molding have begun from the early 1990s. Most researchers found the microstruc-

ture and behaviors of the material (e.g., birefringence, cooling stress, density distribution, and shrinkage of the crystalline plastics) to be dependent on the injection and cooling process. Therefore, the early researchers supplemented the analysis of the heat transfer and the phase transition in injection molding,<sup>6</sup> the mathematical simulation of the temperature distribution after solidification,<sup>4,7,8</sup> and the variational temperature distribution of melting material in injection machine barrel.<sup>5</sup> Masa<sup>9</sup> investigated the cooling process of a slab of crystalline plastic. Ji and Li and their colleagues<sup>10–15</sup> studied the cooling time in injection molding and found a rough model with which to simulate the cooling time of crystalline plastics. Each of these studies has dealt only with specific types of cooling processes. In fact, the injection temperature of crystalline plastics directly influences the degree of crystallinity. A more realistic model is needed to explain the cooling process in injection molding. The present study gives an exact solution for the temperature distribution and the rate of phase change in a slab injection mold. This model was tested with a plastic injection molding machine. Measurements of temperature profiles compare well with model prediction.

## MATHEMATICAL MODEL OF HEAT TRANSFER

### Injection molding setup

A two-dimensional schematic diagram of a mold shape is shown in Figure 1. The polymer melt is injected between two fairly thick steel plates, crystallized for water cooling. When the polymer melt is injected, the polymer melt that contacts the mold wall is solidified in a moment. Two solid–liquid interphases

Correspondence to: X.-r. Fu (f4x1r7@163.com).

Contract grant sponsor: Special Funds for Major Basic Research; contract grant number: 2005CB623808.

Contract grant sponsor: National Natural Science Foundation Commission of China; contract grant number: 10590351.

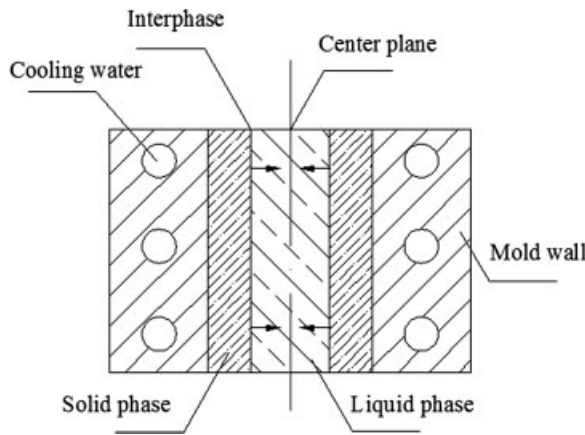


Figure 1 Solidification of a slab. Two-region problem.

appear near the mold wall with the released latent heat. These interphases move to the center plane of the cavity with the same speed. When they disappear at the center plane, the polymer melt is solidified completely. Until the specimen is cooled to the right temperature, it is taken out after opening the mold. The rectangular cavity dimensions in the mold are 150-mm length, 10-mm width, and 4-mm thickness.

**Assumption**

The following assumptions seem reasonable for the cooling system:

1. No fill or flow time: In most polymer injection molding processes, the fill or flow time is significantly less than the total cooling time<sup>16</sup> so flow can be neglected in the system. When polymer melt is injected into the cavity, they begin solidifying.
2. Polymer crystallization: It is initially at a constant temperature  $T_i$ .
3. Intimate contact of surface between the polymer and the mold wall: This is assumed for a valid continuity of the temperature at the surface.<sup>17</sup> Negligible convective heat transfer is considered. The mold wall and the polymer surface have a constant temperature  $T_0$ .
4. One-dimensional heat conduction: Most molded parts are thin in one dimension, and the heat transfer can be reduced to a slab calculation.
5. Half-region of the cavity: This region is studied because the mold and cavity are symmetrical. In our research, the thickness of the specimen is 2 mm.
6. Crystalline plastic polymer: Its transformation temperature is the crystallization temperature  $T_c$ .
7. Constant properties  $\alpha_s, \alpha_l, \rho_s, \rho_l, C_{ps}, C_{pl}$  of polymer: Material properties, thermal diffusivity, density and heat capacity of polymer are assumed constant to simplify the calculation.<sup>18,19</sup>

**Mathematical model derivative process and the solution**

According to the cooling characteristic and the low coefficient of the thermal conductivity of crystalline plastics, the mathematical model could be presented to describe the temperature distribution. First, consider a center plane that is initially at a constant temperature higher than the crystallization temperature in the liquid phase. The temperature of one surface of the slab is instantaneously dropped and remains at a constant temperature  $T_0$ . Solidification is assumed to take place at one temperature. Figure 2 shows the geometry and the temperature profiles.

Thus, with these assumptions, the basic equations of this system can be written as follows:

*Solid phase:*

$$\frac{\partial^2 T_s}{\partial x^2} = \frac{1}{\alpha_s} \frac{\partial T_s(x,t)}{\partial t} \quad 0 < x < S(t), \quad t > 0 \quad (1)$$

$$T_s(x,t) = T_0 \quad x = 0, \quad t = 0 \quad (2)$$

*Liquid phase:*

$$\frac{\partial^2 T_l}{\partial x^2} = \frac{1}{\alpha_l} \frac{\partial T_l(x,t)}{\partial t} \quad S(t) < x < L, \quad t > 0 \quad (3)$$

$$\frac{\partial T_l}{\partial x} = 0 \quad x = L, \quad t > 0 \quad (4)$$

*Solid liquid interphase:*

$$T_s = T_l = T_c \quad t > 0, \quad x = S(t) \quad (5)$$

$$K_s \frac{\partial T_s}{\partial x} - K_l \frac{\partial T_l}{\partial x} = \rho_s \gamma \frac{dS(t)}{dt} \quad t > 0, \quad x = S(t) \quad (6)$$

For the temperature distribution in the solid phase ( $S(t) < L$ ), the exact solution for a semi-infinite body is used.<sup>1</sup> Thus,

$$\frac{T_s - T_0}{T_c - T_0} = \frac{1}{\text{erf}(\lambda_c)} \text{erf}\left(\frac{x}{\sqrt{4\alpha_s t}}\right) \quad S(t) < L \quad (7)$$

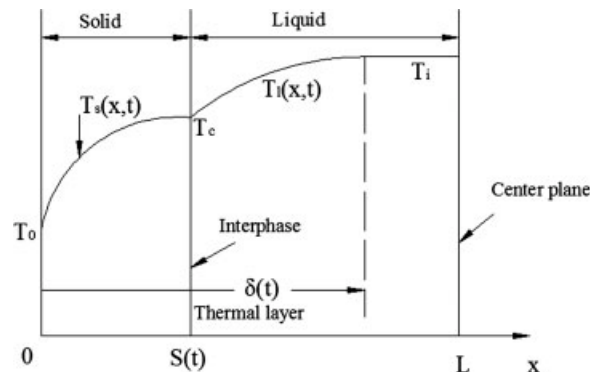


Figure 2 Temperature distribution in a slab injecting mold.

TABLE I  
Parameters for HDPE

$\rho_s$ (kg/m <sup>3</sup> )	$\rho_l$ (kg/m <sup>3</sup> )	$K_s$ (w/m°C)	$K_l$ (w/m°C)	$C_{ps}$ (J/kg°C)	$C_{pl}$ (J/kg°C)	$\alpha_s$ (wm <sup>2</sup> /J)	$\alpha_l$ (wm <sup>2</sup> /J)	$T_c$ (°C)	$\gamma$ (kJ/kg)
954 <sup>a</sup>	785.7 <sup>b</sup>	0.3472 <sup>b</sup>	0.25 <sup>b</sup>	2250 <sup>b</sup>	2250 <sup>b</sup>	$1.8 \times 10^{-7b}$	$1.4 \times 10^{-7b}$	116.4 <sup>c</sup>	160.6 <sup>c</sup>

<sup>a</sup> Values are provided by the manufacturer (DaQing Petroleum Chemical Co., China).

<sup>b</sup> These values are taken from Woo et al.<sup>22</sup>

<sup>c</sup> Values taken from DSC crystallization experiment.

where erf( $x$ ) denotes the complementary error function. It is assumed that the location of the solid-liquid interphase is given by  $S(t) = \lambda\sqrt{4\alpha_s t} = 2\lambda\sqrt{\alpha_s t}$ , where  $\lambda$  is to be determined by solving eqs. (5)–(7).

The integral method is now used to determine the temperature distribution  $T_l(x,t)$  for the liquid phase. To apply the integral method, a thermal layer  $\delta(t)$  is chosen as illustrated in Figure 2. For the finite region considered in this study, the thermal layer concept is valid as long as  $\delta(t) \leq L$ ; it loses its physical significance for  $\delta(t) > L$ . The liquid phase temperature distribution ( $\delta(t) < L$ ) could be given as

$$\frac{T_l - T_i}{T_0 - T_i} = \left( \frac{\delta(t) - x}{\delta(t) - S(t)} \right)^n \cdot \frac{T_c - T_i}{T_0 - T_i} \quad (n = 3), \quad \delta(t) \leq L \quad (8)$$

where  $\delta(t) = \beta\sqrt{4\alpha_s t} = 2\beta\sqrt{\alpha_s t}$ , with  $\beta$  an undetermined coefficient. It is obtained by solving eqs. (5, 6, 8).

The liquid phase temperature distribution ( $\delta(t) = L$ ,  $S(t) < L$ )<sup>20</sup> could be given as

$$T(X, \tau) = T(1, \tau) \left[ 1 - \left( \frac{X - \xi}{1 - \xi} \right)^2 \right] \quad \delta(t) = L \quad S(t) < L \quad (9)$$

where  $X = x/L$ ;  $\xi = S/L$ ;  $\tau = \alpha_s t/L^2$

$$a = \frac{(n+1)\alpha_l}{2\alpha_s\lambda^2} = \frac{3\alpha_l}{2\alpha_s\lambda^2}; \quad \xi = 2\lambda\sqrt{\tau}$$

The temperature at the center plane,  $T(1, \tau)$  can be obtained from

$$T(1, \tau) = T_c + \left( \frac{1 - S_0}{1 - \xi} \right)^{(1+a)} \exp \left[ a \left( \frac{1}{1 - S_0} - \frac{1}{1 - \xi} \right) \right] \quad (T_i - T_c) \quad (10)$$

where  $S_0 = \lambda/\beta$ .

The solid phase temperature distribution ( $S(t) = L$ ) could be given as

$$T_s(x, t) = T_0 + b(t)L \left[ \frac{x}{L} - \frac{1}{3} \left( \frac{x}{L} \right)^3 \right] \quad S(t) = L \quad (11)$$

where  $b(t) = [1.5(T_c - T_0)/L] \exp[12\alpha_s/5L^2(t_{2e} - t)]$ ,  $t_{2e}$  is the time when all the polymer melt is solidification.

## EXPERIMENTAL

### Material

The material used in the experiment was high density polyethylene (HDPE), commercially known as 5000S (DaQing Petroleum Chemical Co., Heilongjiang, China), with an Mn of  $\sim 5.28 \times 10^5$  g mol<sup>-1</sup> and a melt flow rate of 0.90g (10 min)<sup>-1</sup> at 230°C under a force of 21.6N. Transient analysis for HDPE material in a rectangular cavity is selected as case study. The properties of the HDPE material are listed in Table I.<sup>22</sup>

### Experimental procedures

Experiments were carried out on a PS40E 5ASI injection-molding machine. The rectangular cavity dimensions in the mold are 150-mm length, 10-mm width, and 4-mm thickness (Fig. 3). To keep the mold temperature as uniform as possible, a cavity temperature controller with heated circulating water was used. Injection temperature was 234°C. The mold temperature was regulated at 30°C. The injection time was 1.75 s. There was no packing time. A Cu-Constantan thermocouple, of 0.3-mm diameter, was used to record temperature at one position in the mold: the center of the polymer slab ( $X = 2$  mm). Temperature change in the whole process at the center position was recorded with a Keithley 2700 recorder. The interval sampling time was 0.1 s.

## RESULTS AND DISCUSSION

### Theoretical results of temperature distribution

The boundary conditions of this analysis model are shown in Table II. Table III shows the position of

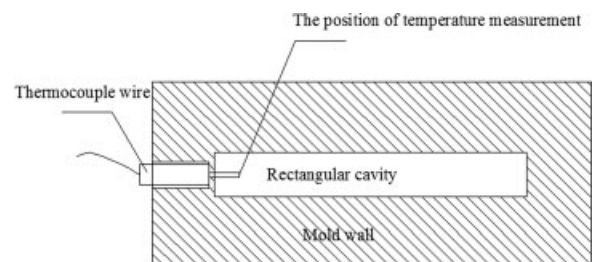


Figure 3 Two-dimensional schematic diagram of an injection mold.

**TABLE II**  
Process Conditions

Injection temperature $T_i$ (°C)	Mold wall temperature $T_0$ (°C)	Position of temperature measurement
234	30	Center of the polymer slab ( $x = 2$ mm)

solid liquid interphase  $S(t)$  and the position of isothermal thermosphere layer interphase at  $\delta(t)$  various times for  $\delta(t) < L$ .

Figure 4 shows the temperature distribution of the whole process. The curves of numbers 1–3 show the temperature distribution for  $\delta(t) < L$ . The time when the thermal layer moves to the center plane is  $t_{1f} = 1.78s$ . 4–7 is the temperature distribution for  $\delta(t) = L$  and  $S(t) < L$ . When  $t_{2e} = 17.11s$ , all the polymer melt is solidification. 8–11 are the curves for  $S(t) = L$ . At last we calculate the demolding time to be  $t_{3f} = 57.56s$ .

**Experimental results and comparison**

Figure 5 presents a comparison of theoretical and experimental temperature profiles as a function of time. For  $t < t_{2e}$  the experimental temperature profile compares well with the model prediction profile. When  $t = t_{2e}$ , both the theoretical and experimental temperature profiles have a horizontal line segment. When the liquid phase temperature drops to 116.4°C, the polymer melt does not solidify at the moment. Then the polymer melt releases the latent heat and solidifies. Until the liquid phase translated into the solid phase, the temperature continues to drop. We come to the conclusion that because of the low coefficient of thermal conductivity of polymer, some of the released latent heat cannot be transferred and the temperature remains unchanged. The theoretical and experimental temperature profiles have a little difference for  $t > t_{2e}$ . One reason is that we assume the intimate contact of surface between the polymer and the mold wall, but in fact the polymer will shrink in solidification.<sup>21</sup> The realistic coefficient of thermal conductivity is lower than the theoretical one. Another reason is that the polymer will crystallize for  $t > t_{2e}$ . The heat of crystallization will release in this time. The experimental rate of cooling is slower than the theoretical one. These two reasons result in the difference in the two profiles for  $t > t_{2e}$ .

**TABLE III**  
Position of  $S(t)$  and  $\delta(t)$  at Various Times for  $\delta(t) \leq L$

$t, s$	0	0.3	0.8	1.51
$S(t), mm$	0	0.257315	0.420194	0.577289
$\delta(t), mm$	0	0.892884	1.458074	2.000000

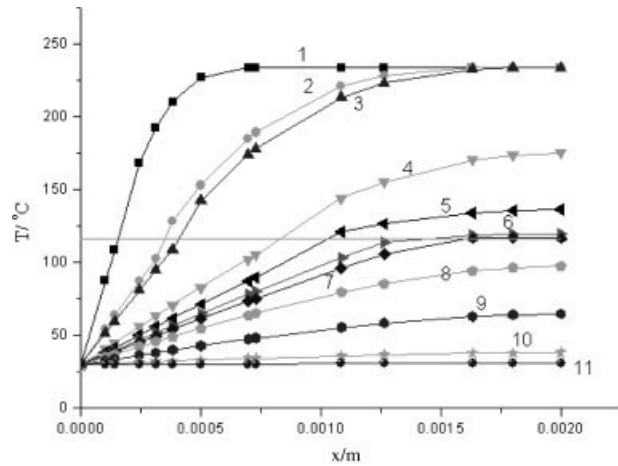


**Figure 4** Temperature distributions of the whole process.

**CONCLUDING REMARKS**

In the present work a mathematical model has been found to explain the cooling process of the injection molding. Especially characteristic of this model is  $t_{1f} < t < t_{2e}$ , which could describe the drop of center plane temperature. A more realistic model proves to be capable of handling problems in the cooling process of injection molding. The temperature distribution during the cooling process can be concluded with the use of this mathematical model. A slight difference is shown for  $t > t_{2e}$  for the theoretical and experimental temperature profiles because the shrinkage of polymer and the heat of crystallization influence the heat transfer. Considering the uncertainty in the physical property measurements and the many assumptions of the model, it may be said that the agreement between experiment and theory is quite good. The results of investigations as well as statistical analyses

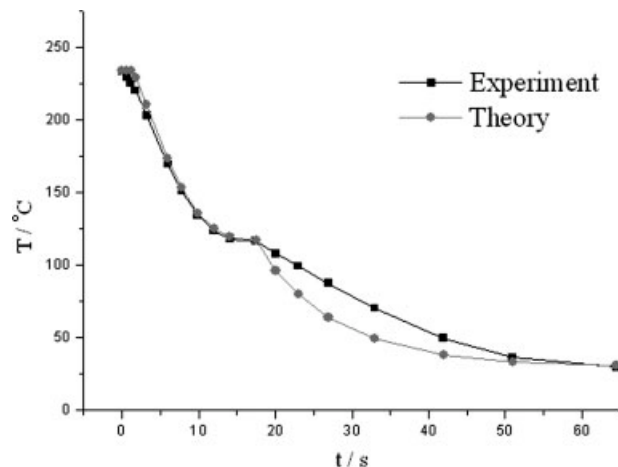


**Figure 5** Comparison of theoretical and experimental temperature profiles as function of time (the temperature recorded is at the center of the polymer slab ( $X = 2$  mm)).

may find their application helpful in optimization activities for injection molding process.

### NOMENCLATURE

$\alpha_s$	thermal diffusivity of solid, $\text{wm}^2/\text{J}$
$\alpha_l$	thermal diffusivity of liquid, $\text{wm}^2/\text{J}$
$K_s$	thermal conductivity of solid, $\text{w}/\text{m}^\circ\text{C}$
$K_l$	thermal conductivity of liquid, $\text{w}/\text{m}^\circ\text{C}$
$C_{ps}$	heat capacity of solid phase, $\text{J}/\text{kg}^\circ\text{C}$
$C_{pl}$	heat capacity of liquid phase, $\text{J}/\text{kg}^\circ\text{C}$
$\rho$	density, $\text{kg}/\text{m}^3$
$\rho_s$	density of solid phase, $\text{kg}/\text{m}^3$
$\rho_l$	density of liquid phase, $\text{kg}/\text{m}^3$
$\gamma$	latent heat of crystallization, $\text{kJ}/\text{kg}$
$T$	temperature, $^\circ\text{C}$
$T_i$	initial temperature, $^\circ\text{C}$
$T_c$	crystallization temperature, $^\circ\text{C}$
$T_s$	solid temperature, $^\circ\text{C}$
$T_l$	liquid temperature, $^\circ\text{C}$
$T_0$	demolding temperature, $^\circ\text{C}$
$S(t)$	the position of solid liquid interphase
$\delta(t)$	the position of isothermal thermosphere layer interphase
$\lambda$	constant defined by $S(t) = \lambda\sqrt{4\alpha_s t} = 2\lambda\sqrt{\alpha_s t}$
$\beta$	constant defined by $\delta(t) = \beta\sqrt{4\alpha_s t} = 2\beta\sqrt{\alpha_s t}$
$L$	thickness of slab, mm
$x$	distance in thickness direction, mm
$X$	dimensionless distance, $x/L$
$t$	time, s
$t_{1f}$	time when the thermal layer move to the center plane, s
$t_{2e}$	time when all the polymer melt is solidification, s
$t_{3f}$	demolding time, s

$\xi$	position of phase change $S(t)/L$ , dimensionless, $\xi(\tau) = 2\lambda\sqrt{\tau}$
$\tau$	dimensionless time, $\alpha_s t/L^2$
$a$	constant defined by $a = \frac{(n+1)\alpha_l}{2\alpha_s\lambda^2} = \frac{3\alpha_l}{2\alpha_s\lambda^2}$
$b$	constant defined by $b(t) = \left[\frac{1.5(T_c - T_0)}{L}\right] \exp\left[\frac{12\alpha_s}{5L^2}(t_{2e} - t)\right]$

### References

1. Goodman, T. R. J. Heat Transfer 1961, 83c, 83.
2. Gage, G. H.; Boyce, D. R. Mass Heat Transfer Phenomon Metall Eng 1973, 9, 368.
3. Heat Transfer Handbook; Federal Republic of Germany Engineer Association Craft and Chemical Engineering Academic Society: Berlin, 1977, p 97.
4. Hu, J. Q.; Li, D. Q. Chin Plast 1995, 9, 5, 52.
5. Nishimura, T. Int Chem Eng 1985, 25, 105.
6. Sqmbatsompop, N. Adv Polym Technol 2000, 19, 79.
7. Guo, Z. Y.; Li, D. Q. Chin Plast 1999, 10, 82.
8. Chen, J. B.; Shen, C. Y. Polym Mater Eng 1995, 11, 1, 95.
9. Masa, I. Plastic 1967, 18, 4.
10. Ji, X. L.; Su, Y. Chin Plast 1995, 9, 37.
11. Huang, R. Chin Plast 1997, 11, 4, 53.
12. Ouyang, W. B.; Huang, R. Plast Ind 2000, 28, 23.
13. Li, H. M.; Gu, Y. X. Chin Plast 1999, 13, 74.
14. Gu, J. Y.; Chen, Y. Insulation Mater Commun 1999, 3, 26.
15. Wang, X. S. Polym Mater Eng 1997, 11, 4.
16. Broyer, E. B.; Macoskoso, C. W. AIChEJ 1976, 122, 268.
17. Carslaw, H. S.; Jaeger, J. C. Conduction of Heat in Solids, 2nd ed.; Oxford University Press: London, 1959.
18. Van Krevelan, D. W. Properties of Polymers; Elsevier: Amsterdam, the Netherlands, 1972.
19. Brandrup, J.; Immergut, E. H. Polymer Handbook; Wiley: New York, 1975; p 7.
20. Cho, S. H.; Sunderland, J. E. J Heat Transfer 1969, 421.
21. Postawa, P.; Koszkul, J. J Mater Processing Technol 2005, 109, 162, 109.
22. Woo, M. W.; Wong, P.; Tang, Y.; Triacca, V.; Gloor, P. E.; Hrymak, A. N.; Hamielec, A. E. Polym Eng Sci 1995, 35, 151.